

# Online Research @ Cardiff

This is an Open Access document downloaded from ORCA, Cardiff University's institutional repository: <https://orca.cardiff.ac.uk/id/eprint/98036/>

This is the author's version of a work that was submitted to / accepted for publication.

Citation for final published version:

Valbuena-Ureña, E., Soler-Membrives, A., Steinfartz, S., Orozco Ter Wengel, Pablo ORCID: <https://orcid.org/0000-0002-7951-4148> and Carranza, S. 2017. No signs of inbreeding despite long-term isolation and habitat fragmentation in the critically endangered Montseny brook newt (*Calotriton arnoldi*). *Heredity* 118 (5) , pp. 424-435. 10.1038/hdy.2016.123 file

Publishers page: <http://dx.doi.org/10.1038/hdy.2016.123>  
<<http://dx.doi.org/10.1038/hdy.2016.123>>

Please note:

Changes made as a result of publishing processes such as copy-editing, formatting and page numbers may not be reflected in this version. For the definitive version of this publication, please refer to the published source. You are advised to consult the publisher's version if you wish to cite this paper.

This version is being made available in accordance with publisher policies.

See

<http://orca.cf.ac.uk/policies.html> for usage policies. Copyright and moral rights for publications made available in ORCA are retained by the copyright holders.



**No signs of inbreeding despite long term isolation and habitat fragmentation in the critically endangered Montseny brook newt**

Valbuena-Ureña E<sup>1,2\*</sup>, Soler-Membrives A<sup>1\*</sup>, Steinfartz S<sup>3</sup>, Orozco-terWengel P<sup>4</sup>, Carranza S<sup>5</sup>

<sup>1</sup>Unitat de Zoologia, Facultat de Biociències, Universitat Autònoma de Barcelona, 08193 Cerdanyola del Vallès (Barcelona), Catalonia, Spain.

<sup>2</sup>Centre de Fauna Salvatge de Torreferrussa (Catalan Wildlife Service – Forestal Catalana). Finca de Torreferrussa, Crta B-140, Km 4,5. 08130, Santa Perpètua de la Mogoda, Barcelona, Spain.

<sup>3</sup>Zoological Institute, Department of Evolutionary Biology, Technische Universität Braunschweig, Mendelssohnstr. 4, 38106 Braunschweig, Germany.

<sup>4</sup>School of Biosciences, Cardiff University, Cardiff, United Kingdom.

<sup>5</sup>Institute of Evolutionary Biology (CSIC-Universitat Pompeu Fabra), Passeig Marítim de la Barceloneta 37-49, 08003 Barcelona, Catalonia, Spain.

Keywords for indexing purposes

*Calotriton arnoldi*, genetic diversity, population structure, critically endangered, conservation genetics, effective population size

Word counts: 7842

\*Corresponding authors

Valbuena-Ureña E

Unitat de Zoologia, Facultat de Biociències, Universitat Autònoma de Barcelona, 08193 Cerdanyola del Vallès (Barcelona), Catalonia, Spain

25 [Emiliojavier.Valbuena@uab.cat](mailto:Emiliojavier.Valbuena@uab.cat)

26 Soler-Membrives A

27 Unitat de Zoologia, Facultat de Biociències, Universitat Autònoma de Barcelona, 08193

28 Cerdanyola del Vallès (Barcelona), Catalonia, Spain

29 [Anna.Soler@uab.cat](mailto:Anna.Soler@uab.cat)

30

31 Running title: Consequences of habitat fragmentation

32

33 **Abstract**

34 Endemic species with restricted geographic ranges potentially suffer the highest risk of  
35 extinction. If these species are further fragmented into genetically isolated  
36 subpopulations, the risk of extinction is elevated. Habitat fragmentation is generally  
37 considered to have negative effects on species survival, despite some evidence for  
38 neutral or even positive effects. Typically, non-negative effects are ignored by  
39 conservation biology. The Montseny brook newt (*Calotriton arnoldi*) has one of the  
40 smallest distribution ranges of any European amphibian (8 km<sup>2</sup>), and is considered  
41 critically endangered by the IUCN. Here, we apply molecular markers to analyze its  
42 population structure, and find that habitat fragmentation due to a natural barrier has  
43 resulted in strong genetic division of populations into two sectors, with no detectable  
44 migration between sites. Although effective population size estimates suggest low  
45 values for all populations, we found low levels of inbreeding and relatedness between  
46 individuals within populations. Moreover, *C. arnoldi* displays similar levels of genetic

diversity to its sister species *C. asper*, from which it separated around 1.5 million years ago and which has a much larger distribution range. Our extensive study shows that natural habitat fragmentation does not result in negative genetic effects, such as the loss of genetic diversity and inbreeding on an evolutionary time scale. We hypothesize that species in such conditions may evolve strategies (e.g. special mating preferences) to mitigate the effects of small population sizes. However, it should be stressed that the influence of natural habitat fragmentation on an evolutionary time scale should not be conflated with anthropogenic habitat loss or degradation when considering conservation strategies.

## **Introduction**

Among threatened species, those that are endemic to a restricted spatial area should *per se* experience a higher risk of extinction. Such risk derives from either stochastic environmental processes (e.g. extreme climatic conditions, fires, etc.), or effects of genetic drift and inbreeding (Allendorf & Luikart 2007). Consequently, the preservation of genetic diversity is important for maintaining the evolutionary (adaptive) potential to overcome environmental changes and enable the population growth and survival that is crucial for the fitness of a species (Allentoft & O'Brien 2010). In general, fragmentation of a species range into smaller subunits by external factors such as anthropogenic activities (Blank *et al.* 2013; Storfer *et al.* 2013) or climatic events (Veith *et al.* 2003) reduces gene flow and compromises the population's long term survival (Sunny *et al.* 2014). A central goal of conservation biology is to identify the genetic structure and diversity of species at the population level (Apodaca *et al.* 2012 and references therein), and characterize the gene flow between populations in relation to the species' dispersal

propensity (i.e. the probability of dispersal between habitat patches) and rates (Slatkin 1994). Organisms with lower dispersal rates are more susceptible to isolation than those with higher dispersal rates. Thus, dispersal may counteract the loss of gene flow among populations and, therefore, has been shown to be an important factor for the long-term survival of species (Allentoft & O'Brien 2010).

Strong genetic differentiation among populations is a sign of interrupted gene flow, with non-natural external factors such as human-induced disturbance causing habitat fragmentation and hindering dispersal (Templeton *et al.* 1990). However, strong differentiation can also be the outcome of non-human mediated processes, such as naturally occurring habitat fragmentation, local adaptation (e.g. Nosil *et al.* 2009; Steinfartz *et al.* 2007) or incipient speciation on a small spatial scale (e.g. MacLeod *et al.* 2015). While it has been generally argued that fragmentation can lead to isolation and thus increase extinction risks, it has also been suggested that in some instances habitat fragmentation can have neutral or even positive effects (Fahrig 2003). A fragmented species may develop populations which individually harbor low levels of genetic variation, but when all populations are considered together, the species does not present low levels of diversity. Consequently, fragmented species may preserve high levels of total genetic variation, similar to equally sized species with panmictic population (Templeton *et al.* 1990).

Amphibians are generally considered to have limited dispersal abilities, causing genetic differentiation across small geographic scales (Monsen & Blouin 2004 and references therein), although more recent studies indicate that in some cases, dispersal propensities have been vastly underestimated (e.g. Smith & Green 2005). The notable sensitivity of amphibians to environmental change and habitat fragmentation are other factors that may reinforce patterns of sharp genetic discontinuation over short distances

(Savage *et al.* 2010; Storfer *et al.* 2013; Velo-Antón *et al.* 2013). Therefore, data on gene flow between populations of endangered amphibians should have a direct influence on management programs and decisions regarding conservation strategies, such as determining the number of breeding lines and translocation actions (Sunny *et al.* 2014).

The genus *Calotriton* (Gray, 1858 and recently resurrected by Carranza & Amat 2005), includes only two species, both inhabiting the Iberian Peninsula and adapted to live in cold and permanent-flowing streams: the Pyrenean brook newt (*C. asper*) and the Montseny brook newt (*C. arnoldi*). *Calotriton asper* is widely distributed across the Pyrenean mountain chain, with some populations extending northwards and southwards, reaching the Pre-Pyrenees, and occupying an area larger than 20,000 km<sup>2</sup>. In contrast, *C. arnoldi* is only known from the Montseny Natural Park in the NE Iberian Peninsula, and its disconnected populations are found within a restricted altitudinal range in seven geographically proximate brooks. Although the historic range of this species is unknown, it currently occupies a total area of only 8 km<sup>2</sup>. Moreover, its habitat is naturally fragmented into two watersheds, on the eastern and western sectors of the Tordera River valley, separated by unsuitable terrestrial habitat between them (see Figure 1A). The current census population size of this species is estimated to be less than 1,500 adult individuals (Carranza & Martínez-Solano 2009). Additionally, recent human activities (e.g. extraction of large amounts of water for commercial purposes, deforestation and the building of forest tracks and roads) have had a significant negative effect on *C. arnoldi*'s habitat (Amat *et al.* 2014). Hence, *C. arnoldi* is among of the most spatially restricted and endangered vertebrates in Europe, and it is classified as critically endangered by the International Union for Conservation of Nature (IUCN) (Carranza & Martínez-Solano 2009).

A previous study based on mitochondrial (Cyt *b*) and nuclear (RAG-1) sequences, as well as morphological characters suggested a high degree of differentiation between populations in the eastern and western sectors of *C. arnoldi*'s distribution range (Valbuena-Ureña *et al.* 2013). Therefore, the observed fragmentation of this species into highly genetically isolated populations is probably the result of an ancient, naturally driven, intrinsic fragmentation process rather than the result of recent human disturbances. However, a detailed exploration of population structure, gene flow among populations, and estimates of ancient and current effective population sizes is lacking. Such studies are crucial for the understanding of past and ongoing evolutionary processes, and their implications for the conservation of such a spatially restricted endemic species.

Although there exists several studies of species with very limited distribution ranges (e.g. Sunny *et al.* 2014), as well as of amphibians with highly structured populations (Blank *et al.* 2013; Blouin *et al.* 2010; Monsen & Blouin 2004; Savage *et al.* 2010), *C. arnoldi* represents an exceptional example of a critically endangered amphibian species with limited dispersal capabilities inhabiting a very small fragmented habitat. Here, we present an analysis of the genetic diversity and evolutionary history of *C. arnoldi* which provides general insights into management priorities of species with a very limited distribution range. In order to estimate the effects of natural habitat fragmentation for this species in terms of fitness related genetic parameters (e.g. genetic diversity, inbreeding coefficients, etc.), we compared these parameters directly in populations from the non-fragmented range of sister species *C. asper* in the central Pyrenees. We discuss the absence of anticipated negative consequences for these parameters in *C. arnoldi* in the light of species conservation in naturally fragmented species.

## Material and methods

### *Sampling and DNA extraction*

A total of 160 adult *C. arnoldi* were analyzed, including samples from all seven known locations of this species (Figure 1A). In recognition of the low dispersal capacity (Carranza & Martínez-Solano 2009) and the absence of migrants between sites (see Results below), individuals from the seven locations are considered herein as demographic populations. Genetic populations will be referred to henceforth as clusters. For conservation reasons, the three eastern populations are herein referred to as A1, A2, A3, and the four western populations as B1, B2, B3 and B4. Samples included 77 individuals from the eastern sector (23 from A1, and 27 from each A2 and A3 populations) and 83 individuals from the western sector (25 from B1, 28 from B2, 26 from B3 and 4 from B4). The small number of individuals from B4 is due to the low abundance of individuals at this site. Therefore, results from this population should be treated with caution. Tissue samples consisted of small tail or toe clips preserved in absolute ethanol. Genomic DNA was extracted using the Qiagen™ (Valencia, California) DNeasy Blood and Tissue Kit, following the manufacturer's protocol.

### *Phylogenetic analyses and estimation of divergence times*

A dataset of mitochondrial and nuclear genes was assembled to estimate the divergence times between *C. asper* and *C. arnoldi*, as well as between *C. arnoldi*'s populations. This dataset consisted of three samples of *C. asper* from Irati, northwestern Pyrenees,



Spain (see Milá *et al.* 2010), and a randomly selected set of three samples from each of the seven known wild populations of *C. arnoldi* (Figure 1A, Supplementary Table S1). The following regions of four mitochondrial and three nuclear genes were amplified and sequenced for both strands, totaling 3553 base pairs (bp) (84 variable positions): 374 bp (16 variable) of the mtDNA gene cytochrome *b* (Cyt *b*) using primers Cytb1EuprF and Cytb2EuprR from Carranza & Amat (2005) and conditions as in Carranza *et al.* (2000); 556 bp (42 variable) of the mtDNA gene NADH dehydrogenase subunit 4 (ND4) using primers from Arèvalo *et al.* (1994) and conditions as in Martínez-Solano *et al.* (2006); 370 bp (5 variable) of the mtDNA gene 12S rRNA (12S) and 553 bp (5 variable) of the mtDNA gene 16S rRNA (16S) with the same primers and conditions as in Carranza & Amat (2005); 695 bp (7 variable) of the nucDNA gene proopiomelanocortin (POMC) and 475 bp (3 variable) of the nucDNA gene brain-derived neurotrophic factor (BDNF) using primers and conditions as in Recuero *et al.* (2012); and 530 bp (6 variable) of the nucDNA gene recombination-activating gene 1 (RAG-1) with primers and conditions as in Šmíd *et al.* (2013). GENEIOUS v. R6.1.6 (Biomatters Ltd.) was used for assembling and editing the chromatographs. Heterozygous positions for the nuclear coding gene fragments were identified based on the presence of two peaks of approximately equal height at a single nucleotide site in both strands, and were coded using IUPAC ambiguity codes. The nuclear coding fragments were translated into amino acids and no stop codons were observed. DNA sequences were aligned for each gene independently using the online application of MAFFT v.7 (Katoh & Standley 2013) with default parameters (Auto strategy, Gap opening penalty: 1.53, Offset value: 0.0). In order to optimize the alignment of the ribosomal genes, we did not include any outgroups and used Bayesian methods for inferring the root of the phylogenetic tree (Huelsenbeck *et al.* 2002).

Best-fitting models of nucleotide evolution were inferred using jModeltest v.0.1.1 (Darriba *et al.* 2012) under the Akaike information criterion (AIC) (Akaike 1973). The HKY model was selected for the 12S and 16S genes and the TrN for all the remaining genes. Phylogenetic analyses were performed using BEAST v.1.8.0 (Drummond & Rambaut 2007). For the time calibration, we used the Hauswaldt *et al.* (2014) rate of molecular evolution of the Cyt *b* gene, inferred for the Urodelan genus *Salamandrina*, based on four fossil/geological calibration points. Three individual runs of  $5 \times 10^7$  generations were performed, sampling every 10,000 generations. Models and prior specifications applied were either program defaults or as follows: model of sequence evolution for each gene, as indicated above; substitution models and clock models unlinked; trees linked; coalescent constant size tree prior; random starting tree; strict clock rate for all the partitions. The molecular evolution rate of Hauswaldt *et al.* (2014) was implemented in our analyses in the clock rate prior of Cyt *b* using a Normal distribution centered at 0.0102 subst/site/Myr, and with a standard deviation that captured 95% of the High Probability Density of the posterior reported by Hauswaldt *et al.* (2014) (0.0085 – 0.018 subst/site/Myr). Posterior trace plots and effective sample sizes (ESS) of the runs were monitored in Tracer v1.5 (Rambaut & Drummond 2007) to ensure convergence. The results of the individual runs were combined in LogCombiner, discarding the initial 10% of the samples, and the maximum clade credibility (MCC) ultrametric tree was produced with TreeAnnotator (both provided with the BEAST package). Nodes were considered strongly supported if they received posterior probability (pp) support values  $\geq 0.95$ .

*Microsatellite loci genotyping and basic population genetic parameters*

Individuals were genotyped for a total set of 24 microsatellite loci: 15 specifically developed for *C. arnoldi* (Valbuena-Ureña *et al.* 2014) and nine additional loci originally developed for the closely related sister species *C. asper*, and which cross-amplify successfully in *C. arnoldi* (Drechsler *et al.* 2013). Microsatellite loci were multiplexed in five mixes using the Type-it multiplex PCR (Qiagen). Primer combinations of the five mixes are provided in the supplementary material (Supplementary Table S2). PCR conditions and genotyping of loci followed the descriptions provided in Drechsler *et al.* (2013).

The MICRO-CHECKER software (Van Oosterhout *et al.* 2004) was used to check for potential scoring errors, large allele dropout and the presence of null alleles. Pairwise linkage disequilibrium between loci was checked using the software GENEPOP version 4.2.1 (Rousset 2008). The same program was used to calculate deviations from Hardy-Weinberg equilibrium in each population and for each locus, which provides an exact probability value (Guo & Thompson 1992). Genetic diversity was measured for each sampling site as the mean number of alleles ( $A$ ), observed ( $H_O$ ) and expected heterozygosity ( $H_E$ ) and allelic richness ( $A_r$ ) using FSTAT version 2.9.3.2 (Goudet 1995). The observed number of private alleles for each locus and each population was calculated with GDA (Lewis & Zaykin 2000), and a rarified measure of private allele richness (PAA<sub>r</sub>) was obtained with HP-RARE (Kalinowski 2005). FSTAT was used to estimate the populations' inbreeding coefficients ( $F_{IS}$ ) following Weir & Cockerham (1984).

In order to compare the genetic diversity measures of *C. arnoldi* to its more widely distributed sister species in the central Pyrenees, we used four *C. asper* populations from the study of Drechsler *et al.* (2013) (Figure 1A) as a reference, adding some samples and re-sequencing others for some markers (see Supplementary Table S2).

The genetic diversity estimates in terms of differences in heterozygosity estimates ( $H_E$  and  $H_O$ ) and number of alleles per locus ( $A$ ) between *C. arnoldi* populations (and clusters) and these four populations of *C. asper* were tested pairwise using a nonparametric Wilcoxon signed-rank test, with Bonferroni's correction for multiple comparisons. The inbreeding coefficients  $F_{IS}$  were also estimated for the *C. asper* populations.

#### *Microsatellite-loci derived population structure analysis*

The pairwise population divergence between *C. arnoldi*'s seven sampling localities was estimated with the  $F_{ST}$  as calculated in FSTAT, and with Jost's  $D$  (Jost 2008) using the R package DEMETICS (Gerlach *et al.* 2010). We also used a Bayesian approach to examine population structure of *C. arnoldi* across its distribution range, as implemented in STRUCTURE version 2.3.4 (Pritchard *et al.* 2000). STRUCTURE's Bayesian clustering algorithm assigns individuals to clusters without using prior information on their localities of origin. Settings used included an admixture model with correlated allele frequencies, and the number of inferred clusters ( $K$ ) ranged from one (complete panmixia) to eight (i.e. the number of sample locations plus one). STRUCTURE was run for each value of  $K$  ten times, with one million Markov Chain Monte Carlo (MCMC) iterations, discarding the first 100,000 MCMC steps as burn-in phase. We also ran STRUCTURE with the same parameters for each sector (eastern and western) separately to check for possible genetic substructure within sectors. The optimal number of clusters was inferred using Evanno *et al.* (2005)  $\Delta K$  method, as implemented in STRUCTURE HARVESTER (Earl & vonHoldt 2012). The average from all the outputs of each  $K$  was obtained with CLUMPP version 1.1.2 (Jakobsson & Rosenberg 2007)

and plotted with DISTRUCT version 1.1 (Rosenberg 2004). Additionally, we employed a model-independent clustering approach using GENETIX, version 4.05.2 (Belkhir *et al.* 2004), by performing a factorial correspondence analysis (FCA) on the allelic frequencies obtained for the seven Montseny brook newt populations. This analysis was performed across the distribution range of *C. arnoldi*, as well as in each sector separately to examine the existence of substructure within them. Analysis of molecular variance (AMOVA) was performed in ARLEQUIN 3.5.1.2 (Excoffier & Lischer 2010) by grouping the sampling localities as indicated by STRUCTURE. Isolation by distance (IBD) was evaluated by examining the relationship between geographical and genetic distances between populations with a Mantel test (Mantel 1967). Since the lifestyle of *C. arnoldi* is strictly aquatic (Carranza & Amat 2005), geographic distances were calculated following the watercourse and log-transformed to linearize the relationship between geographic distances and  $F_{ST}$  values (see Rousset 1997). Genetic distances were calculated as  $F_{ST} / (1 - F_{ST})$ , and the significance of matrix correlation coefficients was estimated with 2,000 permutations in ARLEQUIN. Analyses were performed between all sampled populations and by grouping populations by sector using ARLEQUIN.

#### *Analysis of recent gene flow*

Recent gene flow between sectors and populations within sectors were assessed using three programs: GENECLASS 2.0 (Piry *et al.* 2004), STRUCTURE and BIMr (Faubet & Gaggiotti 2008). The Bayesian assignment approach implemented in GENECLASS was used following Paetkau *et al.* (2004). STRUCTURE was rerun to detect migrants by calculating a  $Q$  value, which is the proportion of that individual's ancestry from a

population. An individual is a putative migrant when the  $Q$  value for its origin site ( $Q_o$ ) is lower than the  $Q$  value for its site of assignment ( $Q_a$ ). BIMr was used to estimate migration rates within the last two generations ( $N_{gen} \leq 2$ ) between populations within sectors. BIMr uses a Bayesian assignment test algorithm to estimate the proportion of genes derived from migrants within the last generation, assuming linkage equilibrium and allowing for deviation from Hardy-Weinberg equilibrium. We estimated migration rates among populations within sectors separately. For each analysis, we ran a Markov chain with a burn-in period of 50,000 iterations, followed by 50,000 samples which were collected using a thinning interval of 50. Convergence of the Markov Chain was assessed by repeating the analyses independently five times. Pairwise migration rates between and within populations across runs were averaged.

### *Inference of demographic history*

The effective population size ( $N_e$ ) for each *C. arnoldi* population and cluster resulting from STRUCTURE, and for the four *C. asper* populations, were calculated using three single-sample  $N_e$  estimators: ONeSAMP (Tallmon *et al.* 2008), COLONY version 2.0.4.4 (Jones & Wang 2010), and LDNe version 1.31 (Waples & Do 2008). ONeSAMP employs approximate Bayesian computation (ABC) and calculates eight summary statistics to estimate  $N_e$  from a sample of microsatellite loci genotypes. The analyses were submitted online to the ONeSAMP 1.2 server (<http://genomics.jun.alaska.edu/asp/Default.aspx>). A variety of input priors were tested, with minimum  $N_e$  as low as 2 and maximum  $N_e$  as high as 1000. After convergence of test runs was achieved, the prior distributions were set between a minimum  $N_e$  of 2 and a maximum value of 100 for populations or 500 for clusters. COLONY implements a

maximum likelihood method to conduct sibship assignment analyses, which are used to estimate  $N_e$  under the assumption of random mating. COLONY was run using the maximum likelihood approach for a dioceous/diploid species, with medium length runs and random mating, assuming polygamy for both males and females (as is the case for most salamanders) with no sibship prior. We did not use the option “update allelic frequencies” and other parameters used as default. Finally, LDNe employs a linkage disequilibrium method (Hill 1981) using a jackknife approach to estimate confidence intervals, and assuming a minimum allele frequency of 2% in order to reduce the bias caused by rare alleles.

In order to characterize changes in demographic history, additional analysis was performed in MSVAR version 1.3 (Storz & Beaumont 2002). This analysis was undertaken for all populations with the exception of B4, due to the low sample size. MSVAR uses a Bayesian approach with coalescent simulations to estimate three population demographic parameters: i) the ancestral population size ( $N_t$ ) of a population, ii) its current effective population size ( $N_0$ ), and iii) the time ( $t$ ) at which the change from  $N_t$  to  $N_0$  occurred. Three scenarios, a bottleneck, an expansion and a stable demography, were tested for each population in order to assess whether the posterior distributions of the three parameters of interest were independent of the prior distributions used to run the analyses. As no microsatellite mutation rate for this species has been described, an average vertebrate rate of  $10^{-4}$  was used (Bulut *et al.* 2009), allowing the rate to vary by up to two orders of magnitude above ( $10^{-2}$ ) and below ( $10^{-6}$ ). Prior distributions are shown in supplementary information (Supplementary Table S3). Each MSVAR run consisted of  $4 \times 10^8$  iterations of the MCMC algorithm, discarding the first 25% of the coalescent simulations. Gelman and Rubin’s diagnostic (Brooks & Gelman 1998) was used to assess convergence between the independent

MSVAR runs using the library CODA (Plummer *et al.* 2006) in R. Lastly, the demographic analysis with MSVAR was complimented with bottleneck analyses in Bottleneck v1.2.02 (Piry *et al.* 1999), under the stepwise mutation and the two-phased mutation models with default parameters.

#### *Genetic relatedness of individuals*

In order to measure levels of inbreeding, the software MLRELATE (Kalinowski *et al.* 2006) was used, which estimates the relatedness among individuals within each population. This program is appropriate as it is designed for microsatellite loci, is based on maximum likelihood tests, and considers null alleles. Furthermore, GenAlEx v. 6 (Peakall & Smouse 2006) was used to obtain pairwise relatedness among individuals in each population separately using the  $r_{\text{qg}}$  estimator (Queller & Goodnight 1989). Mean pairwise relatedness values and their 95% confidence intervals estimates (CI) were calculated for the east and west sectors separately, and the statistical differences in mean population-relatedness between populations were assessed with a permutation test following Peakall & Smouse (2006). These CI intervals of  $r_{\text{qg}}$  from the simulations represent the range of  $r_{\text{qg}}$  that would be expected under random mating across all populations within sectors. Population  $r_{\text{qg}}$  values that fell above the expected 95% CI values indicate a higher relatedness than anticipated and are possibly due to reproductive skew, inbreeding, or genetic drift among populations within the same sector. These estimates of genetic relatedness were also computed for the four *C. asper* populations and are used as a reference of non-fragmented populations.

## **Results**



### Estimation of divergence times

Convergence was confirmed by examining the likelihood and posterior trace plots of the three runs with Tracer v.1.5. Effective sample sizes of the parameters were above 200, indicating a good representation of independent samples in the posterior. The phylogenetic relationships are shown in Figure 1B. *Calotriton asper* and *C. arnoldi* form two independent clades, and within *C. arnoldi* there are two well supported reciprocally monophyletic groups that include the populations from the eastern and western sectors. Nevertheless, none of the sampling localities within either of the two sectors were monophyletic, likely indicating a lack of resolution of the gene fragments used, and/or gene flow between the localities in each sector, or the retention of ancestral polymorphisms between sectors. According to the present dating estimates, *C. asper* and *C. arnoldi* diverged approximately 1.76 Mya (95% HPD 1.24 – 2.44 Ma) and the eastern and western sectors of *C. arnoldi* 0.18 Mya (95% HPD 0.08 – 0.30 Ma).

### Genetic diversity

Genetic diversity for each sampled population and cluster obtained from the genetic structure analyses are given in Table 1 (Supplementary Table S4, for locus-specific results). Loci Us3 and Us7 were monomorphic for the populations within the western sector. We further found that some alleles were fixed for some populations: Calarn15906 was found to be monomorphic in population B2, seven loci (Calarn 29994, Calarn06881, Calarn36791, Calarn52354, Calarn31321, Calarn15136 and Us2) were fixed in population B3, and loci Calarn15906 and Ca32 showed no polymorphisms for individuals of population B4. The observed number of alleles per locus ranged from four to 12, with a mean of 7.08, and the mean number of alleles in the eastern and

western populations were 5.50 and 3.96, respectively. There was no sign of linkage disequilibrium between any pair of loci, with the only exception of Calarn02248 and Calarn50748 in population B3 after Bonferroni correction ( $P < 0.00018$ ). Only two loci in two different populations showed signs of null alleles (Us7 in A1 and Ca22 in B1). Private alleles (PA) – defined here as alleles exclusively found in a single population throughout the study site, i.e. the species range – are also listed in Table 1. Populations of the eastern sector had 75 PAs, while the western populations had 38 PAs. Allelic richness (AR) per population ranged from 1.77 to 4.22, and expected heterozygosity ranged from 0.197 to 0.559 (weighted average: 0.441), with the lowest value found in B3 and the highest in A3. No significant departures from Hardy-Weinberg equilibrium ( $P > 0.0003$ ) were found after applying Bonferroni correction. Overall,  $F_{IS}$  was estimated to be 0.380 ( $P = 0.0021$ ), but this parameter did not show values significantly different from zero for each population after applying Bonferroni correction (see Table 1).

Similar levels of genetic diversity were observed between *C. arnoldi* populations or clusters and the four *C. asper* populations (Table 1, Supplementary Table S5). None of the  $F_{IS}$  values were significantly different from zero for these four populations after applying Bonferroni correction. In general, the total number of alleles per locus and expected and observed heterozygosity values were similar between *C. asper* and *C. arnoldi* populations (and clusters). The differences detected in the western sector are mostly due to population B3, which has low levels of genetic diversity. This population showed some significant differences, mainly when compared to *C. asper* populations at Barranco de Valdragás and Ibón de Acherito (Supplementary Table S6). We only found differences in one of the diversity indices explored (A) with two populations (B2 and B4) compared to two out of the four *C. asper* populations. We did not detect differences

in terms of expected nor observed heterozygosities between any *C. arnoldi* and *C. asper* populations but population B3.

#### *Determining population structure*

Population differentiation was significant for each pair of population combinations ( $P < 0.001$ ) for both the  $F_{ST}$  and Jost's D (Table 2).  $F_{ST}$  values between the eastern versus western sector populations ranged from 0.443 to 0.617, and Jost's D values from 0.801 to 0.877. Pairwise comparisons between populations within sectors were much lower, with  $F_{ST}$  and D values within sectors ranging from 0.086 to 0.372 and 0.100 to 0.299, respectively. Population B4 was not included in the  $F_{ST}$  and D estimations due to its low sample size. Populations A3 of the eastern and B3 of the western sector were the most differentiated populations when compared with their respective sector populations.

Consistent with the results of phylogenetic analyses, STRUCTURE revealed two highly distinct genetic clusters corresponding to populations constituting the eastern and the western sectors (Figure 2). The existence of two clusters was highly supported by the analysis of  $\Delta K$  values corresponding to  $K = 2$  (Figure 2B). Some evidence for additional substructure is also indicated by a second weak peak at  $K = 4$ . When each sector was analyzed independently, two clusters were further identified in each sector, grouping A3 separately from A1 and A2, and B3 separately from B1, B2 and B4 (Figure 2A). The same general results were also found with the FCA (Supplementary Figure S1), which demonstrated the clear separation between the two sectors. In these results, A3 and B3 were also the most distinct populations in their respective sectors. The results of the *a posteriori* AMOVA revealed that the clusters resulting from STRUCTURE ( $K=2$ ) explained 40.81% of the molecular variance, 11.61% was

explained by among populations within groups, and 48.31% by within population variation. These results agree with the population differentiation analysis ( $F_{ST}$  values; Table 2).

A relationship between genetic differentiation and geographical distance (Supplementary Table S7) was found among all sampled populations (Supplementary Figure S2,  $r=0.735$ ,  $P = 0.020$ ), suggesting a strong isolation by distance effect at the level of all populations. However, at a finer scale, when both sectors were analyzed independently, no isolation by distance was observed.

#### *Recent gene flow and migration rates*

No migration between the eastern and western sectors could be detected by any of the methods used. All individuals of the eastern sector were assigned by GENECLASS with a probability of 90% or higher to their population of origin. In the western sector, 96% of individuals originating from B1 and 88% of the individuals originating from B3 were correctly assigned to their population of origin. Among the samples from B2, a total of 10.7% of individuals were assigned to B4 and 17.9% to B1, while the remaining 71% of individuals were assigned to their population of origin. About 8.7% of the individuals could not be assigned to any of the sampled populations. No first-generation migrants were detected among populations from the eastern sector, and in the western sector only one individual from B2 was detected to be migrant from B1 ( $P = 0.001$ ). Although this individual had a low probability of being a migrant from B1 (probability of migration of 0.038 according to analysis in STRUCTURE), it had an estimated posterior probability of 0.231 to have a single parent from population B1. STRUCTURE results were similar to GENECLASS assignments, with over 98% of the sampled individuals being assigned

to their population of origin. Estimates of recent gene flow using BIMr were consistent among the five independent runs, suggesting that convergence of the Markov chain had been reached. Recent migration rates showed no detectable recent gene flow between populations within either the eastern or western sectors (Supplementary Table S8). The overall outcome of the recent gene flow and migration rate analyses are in keeping with the population structure detected above.

#### *Demographic history – effective population size ( $N_e$ )*

All three methods used to estimate the effective population sizes ( $N_e$ ) of the seven populations and of the two sectors (i.e. the two clusters identified by Structure) resulted, in general, in low values, ranging from 7 to 342 (see Table 3). Estimation of the 95% CI upper limit for populations A1 and A3 was problematic (estimated at infinity or incongruence values) in the linkage disequilibrium method (LDNe). Despite slight differences between methods, in general all estimators showed narrow CIs, thereby supporting the accuracy of these estimates. Effective population sizes were particularly low in population B3, with a 95% CI estimate of  $N_e = 2 - 30$  regarding the three methods used. Effective population sizes for the *C. asper* populations were similar or higher than those of the *C. arnoldi* populations (Table 3).

Consistent with the previous results, MSVAR analysis also indicated relatively small current  $N_e$  values for each of the six populations tested (B4 was not tested). For all populations, the current effective population size seems to have been the outcome of a reduction in  $N_e$  some time between 1,000 and 10,000 years ago, with the populations' ancestral  $N_e$  being at maximum, one to two orders of magnitude larger than the current one, e.g.  $N_0$  A2  $\sim 100$ ,  $N_t$  A2  $\sim 1,000$  (Figure 3 and Supplementary Table S9). The ratio

of the ancestral  $N_e$  divided by the current  $N_e$  consistently result in values larger than 1 for all populations, providing further evidence for a decrease in  $N_e$  in the past of these populations (Supplementary Figure S3). All MSVAR analyses showed convergent results, as indicated by a Gelman & Rubin statistic being under 1.2, with the exception of the clustered populations identified by STRUCTURE, where the MCMC did not converge. Lastly, analyses performed in BOTTLENECK did not identify a significant excess of heterozygosity in any of the sampled populations (nor in the sectors) (Wilcoxon one tailed test for excess of heterozygosity  $p > 0.05$  for all tests), suggesting that the bottleneck indicated by MSVAR probably did not cause a dramatic loss of genetic diversity.

#### *Relatedness of individuals*

All populations presented a similar proportion of relatedness (Table 3), with most individuals being highly unrelated to each other (80%). The only exception was population B3, which had a lower percentage of unrelated specimens (68%). Full sibling and parent-offspring relations in B3 were 12 and 11%, respectively, while the other populations showed much lower percentages, none exceeding 4%. The estimated Queller & Goodnight (1989) index of relatedness, calculated between individuals in each population separately, indicated random mating among individuals within each population, i.e. panmixia within populations (A1,  $r_{qg} = -0.045$ ; A2,  $r_{qg} = -0.038$ ; A3,  $r_{qg} = -0.038$ ; B1,  $r_{qg} = -0.042$ ; B2,  $r_{qg} = -0.037$ ; B3,  $r_{qg} = -0.067$ ; B4,  $r_{qg} = -0.333$ ). Conversely, at the sector level (i.e. when testing whether there is random mating between populations within a sector), values ranged from 0.150 to 0.206 and from 0.019 to 0.231 within the eastern western sectors respectively, with the only exception being

population B3, which showed an average pairwise relatedness ( $r_{\text{qg}}$ ) of 0.745 (upper and lower CI estimates at 95% of 0.759 and 0.730, respectively). Most populations demonstrated significantly higher relatedness than could be expected if each sector represented a panmictic population. Thus, consistent with our results of the gene flow and migration rate analysis, this suggests random mating among individuals from distinct populations within sectors does not occur (Supplementary Figure S4). These results are concordant with the lack of migration among populations indicated by other analyses. Similar values of relatedness were detected for the reference *C. asper* populations (Table 3) and  $r_{\text{qg}}$  (Ibón de Perramó,  $r_{\text{qg}} = -0.031$ ; Barranco de Valdragás,  $r_{\text{qg}} = -0.026$ ; Ibón de Acherito,  $r_{\text{qg}} = -0.046$ ; Bassies,  $r_{\text{qg}} = -0.005$ ).

## Discussion

Habitat fragmentation is typically expected to lead to a decrease in genetic diversity due to stochastic processes (e.g. genetic drift), which have a stronger effect in smaller populations (Leimu *et al.* 2006). Therefore, species restricted to small geographic areas may experience a high risk of extinction if populations become fragmented and isolated from each other. However, there is also some evidence to suggest that habitat fragmentation can give rise to neutral or even positive effects (Fahrig 2003; Templeton *et al.* 1990). Here we show that extreme subdivision in an amphibian species (*Calotriton arnoldi*) has not negatively affected certain genetic parameters that are supposed to be important indicators for fitness, such as genetic diversity and inbreeding coefficients, when compared to non-fragmented populations of its sister species (*C. asper*).

## Phylogenetic divergence

The estimated divergence between the two species of *Calotriton* confirms previous dating analyses (Carranza & Amat 2005), and indicates that these species split approximately 1.5 Mya, during the Pleistocene epoch. Speciation within *Calotriton* may have been initiated by a geographical barrier, or could have resulted from climatic fluctuations during the Pleistocene. Following the challenging climatic conditions of the last glacial maximum, the high dispersal capabilities of the Pyrenean brook newt helps to explain its rapid dispersion through the Pyrenean axial chain and the Prepyrenees; this allowed the connection of populations and subsequent genetic homogenization as a consequence of gene flow (Valbuena-Ureña *et al.* 2013). In contrast to *C. asper*, a juvenile dispersal phase is absent in *C. arnoldi*, therefore hindering its capacity for colonization. This species probably found refuge in the Montseny massif, being unable to colonize areas beyond the Montseny mountain. The differentiation into two sectors seems to be relatively ancient (~180,000 years ago), coinciding with the Riss glaciation (300,000 – 130,000 ya). This glaciation is characterized by a significant temperature drop and dry climate, which may have decreased the water flow of the Tordera River, causing the extinction of intermediate populations between the current populated sites. Such a scenario is further corroborated by differences in morphology, as well as mitochondrial and nuclear coding genes between the sectors (Valbuena-Ureña *et al.* 2013), suggesting that the fragmentation into subpopulations is not a recent event driven by anthropogenic activities, but rather by natural processes. As our results indicate (Figure 3), the effective population sizes of *C. arnoldi* populations have remained low since the species split.

Neutral genetic diversity is shaped by the balance of evolutionary forces (mutation, genetic drift and migration) over contemporary and historical time-scales



(Dalongeville *et al.* 2016). Although genetic diversity greatly depends on the age of the population concerned, the *Calotriton* species have diverged relatively recently and both have experienced similar historical climatic events (Valbuena-Ureña *et al.* 2013); therefore, the comparison between them is appropriate (Hendrix *et al.* 2010).

#### *Patterns of genetic diversity*

Due to lower vagility, loss of genetic diversity in amphibians is likely to be greater than in many other taxa, and is highly correlated with declines in population fitness and the diminishment of their adaptive potential (Allentoft & O'Brien 2010). Overall, it appears that across its small and restricted distribution range, moderate levels of genetic diversity and high genetic differentiation among sites characterize the Montseny brook newt. The comparison of genetic variation between this species and its closely related and ecologically similar sister species *C. asper* indicates that in general, *C. arnoldi* harbors similar levels of genetic diversity despite its far smaller distribution range. The differences detected in the western sector are mostly due to population B3. We can state that population B3 differs from all other populations of the same species, not only from *C. asper* populations. Therefore, we believe these data do not support a general pattern in which the western sector significantly differs from the four randomly selected *C. asper* populations. It seems that population B3 is an example of a fragile population in terms of low genetic diversity and low effective sizes rather than a situation in which the entire sector suffers the effects of habitat fragmentation. Moreover, neither species show signs of inbreeding. *C. asper* shows similar or slightly higher values of  $N_e$  than *C. arnoldi*. While *C. asper* has a juvenile dispersal phase that may reduce risk of inbreeding, *C. arnoldi* is exclusively aquatic with no dispersal phase, and may therefore have developed other mechanisms to counteract the genetic consequences of small

populations sizes. It is surprising that populations of *C. arnoldi* display similar levels of genetic variation to *C. asper* despite their differences in range size, despite *C. arnoldi* effective population size, and the evidence of a past bottleneck. However, when comparing the expected heterozygosity of *C. arnoldi* to that of other salamanders and temperate amphibians, *C. arnoldi* is within the typical range (0.4 – 0.6; Chan & Zamudio 2009 and references therein).

Our results clearly show that *C. arnoldi* populations are highly structured over short geographic distances, and the species is differentiated into an eastern and a western sector (Figure 2). Interestingly, the eastern sector presents higher levels of genetic variability than the western sector both in terms of microsatellite loci and nuclear and mitochondrial DNA sequences (Valbuena-Ureña *et al.* 2013). The most likely explanation for this pattern is the larger effective population sizes of the eastern populations in comparison to the western ones.

That the two sectors are highly genetically differentiated, with no gene flow between them, is indicated by multiple lines of evidence, including: a large number of private alleles in each sector (75 and 38 in the eastern and western sectors, respectively); significantly different patterns of genetic variation between sectors (e.g. AMOVA, allelic richness and the number of fixed alleles in each sector); outcome of the PCA analysis; high  $F_{ST}$  values; unambiguous genetic assignment of individuals to their population of origin; and observed isolation by distance effect. Since *C. arnoldi* is exclusively aquatic, dispersal can only occur along watercourses, therefore reducing dispersal capabilities with respect to similar species capable of terrestrial dispersal. This is reflected in the levels of genetic differentiation observed, which are notably higher than values typically found for amphibians that use both aquatic and terrestrial habitats (Spear *et al.* 2005). The sectors of *C. arnoldi* are effectively isolated by a 37 km long

watercourse, whereas distance by land is only 6 km. The watercourse between the two sectors passes through long stretches of river which includes a low altitude (<600 m) section with high water temperatures and potential predators; it therefore constitutes an adverse environment for these aquatic newts and thus presents a strong migration barrier. Accordingly, we can assume that in this system, natural fragmentation has played a strong impact on observed and associated microevolutionary processes (see Templeton *et al.* 1990).

Although the strong population subdivision is clearly detected between sectors, the low dispersal capability of this species is also detected among populations within sectors. The significant  $F_{ST}$  values indicate that dispersal between populations is low, as confirmed by the differentiation of populations/clusters A3 and B3 from the other populations within their respective sectors. These results were consistent with the outcome of PCA analysis and migration tests. Moreover, at a sector level, most populations showed significantly higher degrees of relatedness ( $r_{qg}$ ) than expected if sectors were in panmixia. This pattern is expected when migration among populations is not sufficiently high to counteract the relatedness resulting from nonrandom mating among populations. This notable sector structuring could suggest high levels of relatedness and inbreeding of individuals within populations. However, this is not found, as non-relatedness values within populations remain high, and random mating within populations seems to occur (see discussion below).

Our results indicate that the overall genetic diversity of *C. arnoldi* has been maintained at relatively high levels across its small and fragmented distribution range. This species comprises of highly genetically differentiated populations which display moderate levels of genetic diversity. Therefore, both intrapopulation genetic diversity levels and the strong differentiation among them allow this species to retain enough

genetic variation to persist despite the vulnerability inherent in its small distribution range.

#### *The impact of natural fragmentation on C. arnoldi*

It is broadly accepted that habitat fragmentation (either naturally occurring or human driven) will result in the subdivision of populations and, if migration of individuals is not possible, subpopulations will start to diverge genetically (Frankham *et al.* 2010; Templeton *et al.* 1990). However, Templeton *et al.* (1990) suggested that despite the negative effects deriving from fragmentation, genetic variation is not completely lost, but often presents as fixed differences between local populations. Although this aspect is relevant for species conservation, it is little considered at present, and pertinent case studies are lacking. In our view, the surprising results obtained herein, involving an endangered species affected by natural habitat fragmentation, provide an excellent study system to promote discussion on this overlooked aspect.

Both the census and effective population sizes in *C. arnoldi* rank it as a critically endangered species; current  $N_e$  values for all *C. arnoldi* populations are critically low (<50) and are consistent with the small census size (Carranza & Martínez-Solano 2009). The divergence time estimated between *C. asper* and *C. arnoldi*, and between the two *C. arnoldi* sectors, indicates that these splits were not recent events (over 1 Mya the former and over 100 Kya for the latter). Moreover, the  $N_e$  values estimated for *C. arnoldi* indicate a small population size throughout its comparable short evolutionary history of roughly 1.76 Mya. These facts support the hypothesis that after the divergence of the two species, *C. asper* went through a rapid expansion phase, while *C. arnoldi* remained geographically restricted. The current distribution range of *C. asper*

populations cover an area of roughly 20,000 km<sup>2</sup>, while populations of *C. arnoldi* are restricted to an area of only 8 km<sup>2</sup>; such differences are expected to be reflected in genetic parameters, and yet they are not.

In general, different behavioral strategies can be assumed for animals to avoid inbreeding. The most easy and obvious strategy would be postnatal dispersal of individuals to reduce the probability of inbreeding, the second would be mating preferences for non-related individuals (Blouin & Bloiun 1988). Based on the high degree of genetic differentiation and the lack of migration between *C. arnoldi* subpopulations between the two sectors, we can basically exclude postnatal dispersal as a mechanism to avoid inbreeding. It is therefore likely that special mating preferences exist in *C. arnoldi* to minimize the effects of potential inbreeding. As we have not observed an excess of heterozygosity for analysed microsatellite loci across sectors, we can further conclude that females – assuming that they are the choosing sex – might not only prefer to mate with unrelated males but also with related ones. Indeed, more recent empirical studies – in contrast to early ones – indicate that animals sometimes show no avoidance or even prefer to mate with relatives (see Szuklin *et al.* 2013). In crickets, for example, Tregenza & Wedell (2002) could show that females mating multiply with different males avoid low egg viability, which occurs when solely mating with non-related or only with related males, if they mate with both unrelated and related males. Sperm storage in special cloacal glands of the female (called spermathecae) in combination with multiple paternity is widespread and well documented for salamander and newt species of the suborder Salamandroidea, to which also *Calotriton* newts belong (Kühnel *et al.* 2010; Caspers *et al.* 2014). Although we are lacking direct evidence, it is very likely that females of *C. arnoldi* mate multiply with different males, resulting in multiple paternities. Assuming similar mating patterns as described above

for crickets, *C. arnoldi* newts could avoid the negative consequences of inbreeding without displaying an excess of heterozygosity. Of course, at the moment it is completely unclear and needs further investigation by which behavioral mechanisms these newts can cope with small sizes of fragmented populations.

Overall, our results suggest that in terms of maintaining genetic diversity, small effective population sizes do not necessarily pose a problem, as there may be other reproductive or behavioral mechanisms that can counteract the effects of genetic drift (Allentoft & O'Brien 2010). In *C. arnoldi*, such mechanisms are likely to have prevented a substantial loss of alleles through the bottleneck experienced during the Holocene. Evidence suggests that life history strategies can explain a considerable proportion of the variation in genetic diversity, as polymorphism levels are influenced by species biology (Dalongeville *et al.* 2016; Fouquet *et al.* 2015; Paz *et al.* 2015; Romiguier *et al.* 2014). Ecological factors affecting genetic diversity may include migration capability, morphological or physiological adaptations, and reproductive strategy, amongst others.

Our results indicate that the overall genetic diversity of *C. arnoldi* has been maintained at a relatively high level despite its small and fragmented distribution range. Therefore, species fragmentation should not be regarded in this case as primarily detrimental. Populations of *C. arnoldi* do not show the low levels of intrapopulation genetic diversity or signs of inbreeding that are typical byproducts of habitat fragmentation. However, data regarding the potential effect of the fragmentation on a species potential to adapt to environmental changes, which again may be influenced by the life-history strategies, are currently lacking (Dalongeville *et al.* 2016; Romiguier *et al.* 2014). Further studies are needed to understand the relationship between genetic diversity, adaptive potential, and life-history traits in this species.

Species characterized by independent and isolated populations may avoid species-level extinction, since local (population-level) extinctions, resulting from local demographic stochasticity or small-scale environmental catastrophes are unlikely to be simultaneously experienced by all populations. Furthermore, in terms of infectious diseases (e.g. parasite infections or bacterial pathogens such as those causing the “Red-leg” syndrome; Allentoft & O’Brien 2010; Daszak *et al.* 2003), populations that are completely isolated might survive an outbreak since there is little or no exchange of individuals between single populations. Therefore, the persistence of some populations facilitates the survival of the species, and recolonization may occur over time, thus reversing extirpations.

#### *Implications for conservation*

Impacts of habitat fragmentation must be measured independently from effects of habitat loss or degradation. The effects of habitat loss may outweigh the effects of habitat fragmentation, and can have important implications for conservation. Habitat loss is widely recognized to have strong and consistently negative effects on biodiversity, reducing species richness, population abundance and distribution, and genetic diversity (Fahrig 2003 and references therein).

In conservation biology, a  $N_e$  of 500 has been suggested as a minimum value for the long-term survival of a species, whereas  $N_e$  values below 50 in isolated populations are of major concern (Frankham *et al.* 2014), since these populations have an increased probability of extinction resulting from genetic effects like inbreeding (Allendorf & Luikart 2007) and stochastic environmental processes. Inbreeding is exacerbated by small  $N_e$  values. However, it is possible that populations with low  $N_e$  may survive over

long periods of time as they can successfully and rapidly purge detrimental allelic variants, such a scenario has been proposed for other species (e.g. Orozco-terWengel *et al.* 2015). However, the current low effective population sizes of *C. arnoldi* mean that habitat loss or degradation could rapidly drive these small populations to extinction. Stochastic factors can cause a disproportionately high mortality rate when species have very small distribution ranges. Moreover, the effects of habitat loss may be greater when the habitat is highly and rapidly fragmented. This implies that a key question concerning the conservation of a species is “how much habitat is enough?”. The conservation of a vulnerable or endangered species requires estimating the minimum habitat required for persistence of the given species. In addition, many species require more than one kind of habitat within a life cycle. Therefore, landscape patterns that maintain the required habitat proportions should be conserved (Fahrig 2003).

Studies which enhance understanding of genetic population structure and the gene flow between them contribute valuable information to management and conservation programs. The definition of appropriate conservation units are crucial for maintaining the distinct evolutionary lineages and the species’ evolutionary potential (Frankham *et al.* 2010). In *C. arnoldi*, the evolutionary potential is not only manifested within the species as a whole, but also within each sector. Conservation strategies should be adopted to ensure that the evolutionary potential and the genetic diversity within the distinct groups is not lost. Therefore, such strategies should focus on habitat preservation and restoration of each sector, with the aim of maintaining the strong population structure highlighted by this study.

## **Acknowledgements**



We are grateful to all members of the CRFS Torreferrussa, and especially to M. Alonso, F. Carbonell, E. Obon and R. Larios. We also thank the DAAM department of the Generalitat de Catalunya, the staff of Parc Natural del Montseny of the Diputació de Barcelona, and F. Amat. We are very grateful to Amy MacLeod (EditingZoo) for the English editing. This research was supported by Miloca and Zoo de Barcelona (PRIC-2011). S.C. is supported by a grant CGL2012-36970 from the Ministerio de Economía y Competitividad, Spain (co-funded by FEDER). We thank Ralf Hendrix for performing the primary microsatellite loci analysis in the laboratory.

#### **Conflict of interest**

The authors declare no conflict of interests.

#### **Data archiving**

Data deposited in the Dryad repository: xxxxx

#### **References**

- Akaike H (1973) Information theory and an extension of the maximum likelihood principle. In: *Second International Symposium on Information Theory* (eds. Petrov BN, Csaki F), pp. 267-281. Akademiai Kiado, Budapest, Hungary.
- Allendorf FW, Luikart G (2007) *Conservation and the Genetics of Populations* Blackwell, Oxford.
- Allentoft M, O'Brien J (2010) Global amphibian declines, loss of genetic diversity and fitness: a review. *Diversity* **2**, 47-71.

777 Amat F, Carranza S, Valbuena-Ureña E, Carbonell F (2014) Saving the Montseny brook  
778 newt (*Calotriton arnoldi*) from extinction: an assessment of eight years of  
779 research and conservation. *Froglog* **22**, 55-57.

780 Apodaca J, Rissler L, Godwin J (2012) Population structure and gene flow in a heavily  
781 disturbed habitat: implications for the management of the imperilled Red Hills  
782 salamander (*Phaeognathus hubrichti*). *Conservation Genetics* **13**, 913-923.

783 Arèvalo E, Davis SK, Sites JW (1994) Mitochondrial DNA sequence divergence and  
784 phylogenetic relationships among eight chromosome races of the *Sceloporus*  
785 *grammicus* complex (Phrynosomatidae) in Central Mexico. *Systematic Biology*  
786 **43**, 387-418.

787 Belkhir K, Chikhi L, Raufaste N, Bonhomme F (2004) GENETIX 4.05, logiciel sous  
788 Windows TM pour la génétique des populations. Laboratoire Génome,  
789 Populations, Interactions, CNRS UMR 5000: Université de Montpellier II,  
790 Montpellier (France).

791 Blank L, Sinai I, Bar-David S, Peleg N, Segev O, Sadeh A, Kopelman NM *et al.* (2013)  
792 Genetic population structure of the endangered fire salamander (*Salamandra*  
793 *infraimmaculata*) at the southernmost extreme of its distribution. *Animal*  
794 *Conservation* **16**, 412-421.

795 Blouin SF, Blouin M (1988) Inbreeding avoidance behaviours. *Trends in ecology &*  
796 *evolution* **3**, 230-233.

797 Blouin M, Phillipsen I, Monsen K (2010) Population structure and conservation  
798 genetics of the Oregon spotted frog, *Rana pretiosa*. *Conservation Genetics* **11**,  
799 2179-2194.

800 Brooks SP, Gelman A (1998) General methods for monitoring convergence of iterative  
801 simulations. *Journal of Computational and Graphical Statistics* **7**, 434-455.

802 Bulut Z, McCormick C, Gopurenko D, Williams R, Bos D, DeWoody JA (2009)  
803       Microsatellite mutation rates in the eastern tiger salamander (*Ambystoma*  
804       *tigrinum tigrinum*) differ 10-fold across loci. *Genetica* **136**, 501-504.

805 Carranza S, Amat F (2005) Taxonomy, biogeography and evolution of *Euproctus*  
806       (Amphibia: Salamandridae), with the resurrection of the genus *Calotriton* and  
807       the description of a new endemic species from the Iberian Peninsula. *Zoological*  
808       *Journal of the Linnean Society* **145**, 555-582.

809 Carranza S, Arnold EN, Mateo JA, López-Jurado LF (2000) Long-distance colonization  
810       and radiation in gekkonid lizards, *Tarentola* (Reptilia: Gekkonidae), revealed by  
811       mitochondrial DNA sequences. *Proceedings of the Royal Society of London.*  
812       *Series B: Biological Sciences* **267**, 637-649.

813 Carranza S, Martínez-Solano I (2009) *Calotriton arnoldi*. IUCN Red List of Threatened  
814       Species. Version 2012.1

815 Caspers BA, Krause ET, Hendrix R, Kopp M, Rupp O, Rosentreter K *et al.* (2014) The  
816       more the better – polyandry and genetic similarity are positively linked to  
817       reproductive success in a natural population of terrestrial salamanders  
818       (*Salamandra salamandra*). *Molecular Ecology* **23**, 239-250.

819 Chan LM, Zamudio KR (2009) Population differentiation of temperate amphibians in  
820       unpredictable environments. *Molecular Ecology* **18**, 3185-3200.

821 Dalongeville A, Andrello M, Mouillot D, Albouy C, Manel S (2016) Ecological traits  
822       shape genetic diversity patterns across the Mediterranean Sea: a quantitative  
823       review on fishes. *Journal of Biogeography* **43**, 845-857.

824 Darriba D, Taboada GL, Doallo R, Posada D (2012) jModelTest 2: more models, new  
825       heuristics and parallel computing. *Nature Methods* **9**, 772-772.

826 Daszak P, Cunningham AA, Hyatt AD (2003) Infectious disease and amphibian  
827 population declines. *Diversity and Distributions* **9**, 141-150.

828 Drechsler A, Geller D, Freund K, Schmeller DS, Künzel S, Rupp O *et al.* (2013) What  
829 remains from a 454 run: estimation of success rates of microsatellite loci  
830 development in selected newt species (*Calotriton asper*, *Lissotriton helveticus*,  
831 and *Triturus cristatus*) and comparison with Illumina-based approaches. *Ecology*  
832 *and Evolution* **3**, 3947-3957.

833 Drummond A, Rambaut A (2007) BEAST: Bayesian evolutionary analysis by sampling  
834 trees. *BMC Evolutionary Biology* **7**, 214.

835 Earl D, vonHoldt B (2012) STRUCTURE HARVESTER: a website and program for  
836 visualizing STRUCTURE output and implementing the Evanno method.  
837 *Conservation Genetics Resources* **4**, 359-361.

838 Evanno G, Regnaut S, Goudet J (2005) Detecting the number of clusters of individuals  
839 using the software structure: a simulation study. *Molecular Ecology* **14**, 2611-  
840 2620.

841 Excoffier L, Lischer HEL (2010) Arlequin suite ver 3.5: a new series of programs to  
842 perform population genetics analyses under Linux and Windows. *Molecular*  
843 *Ecology Resources* **10**, 564-567.

844 Fahrig L (2003) Effects of habitat fragmentation on biodiversity. *Annual Review of*  
845 *Ecology, Evolution, and Systematics* **34**, 487-515.

846 Faubet P, Gaggiotti OE (2008) A new bayesian method to identify the environmental  
847 factors that influence recent migration. *Genetics* **178**, 1491-1504.

848 Fouquet A, Courtois EA, Baudain D, Lima JD, Souza SM, Noonan BP *et al.* (2015) The  
849 trans-riverine genetic structure of 28 Amazonian frog species is dependent on  
850 life history. *Journal of Tropical Ecology* **31**, 361-373.

851 Frankham R, Ballou JD, Briscoe DA (2010) *Introduction to Conservation Genetics*, 2nd  
852 edn. Cambridge University Press, Cambridge.

853 Frankham R, Bradshaw CJ, Brook BW (2014) Genetics in conservation management:  
854 revised recommendations for the 50/500 rules, Red List criteria and population  
855 viability analyses. *Biological Conservation* **170**, 56-63.

856 Gerlach G, Jueterbock A, Kraemer P, Deppermann J, Harmand P (2010) Calculations of  
857 population differentiation based on GST and D: forget GST but not all of  
858 statistics! *Molecular Ecology* **19**, 3845-3852.

859 Goudet J (1995) FSTAT (Version 1.2): A computer program to calculate F-statistics.  
860 *Journal of Heredity* **86**, 485-486.

861 Guo SW, Thompson EA (1992) Performing the exact test of Hardy-Weinberg  
862 proportion for multiple alleles. *Biometrics* **48**, 361-372.

863 Hauswaldt JS, Angelini C, Gehara M, Benavides E, Polok A, Steinfartz S (2014) From  
864 species divergence to population structure: A multimarker approach on the most  
865 basal lineage of Salamandridae, the spectacled salamanders (genus  
866 *Salamandrina*) from Italy. *Molecular Phylogenetics and Evolution* **70**, 1-12.

867 Hendrix R, Susanne Hauswaldt J, Veith M, Steinfartz S (2010) Strong correlation  
868 between cross-amplification success and genetic distance across all members of  
869 ‘True Salamanders’ (Amphibia: Salamandridae) revealed by Salamandra  
870 salamandra-specific microsatellite loci. *Molecular Ecology Resources* **10**, 1038-  
871 1047.

872 Hill WG (1981) Estimation of effective population size from data on linkage  
873 disequilibrium. *Genetics Research* **38**, 209-216.

874 Huelsenbeck JP, Larget B, Miller RE, Ronquist F (2002) Potential applications and  
875 pitfalls of bayesian inference of phylogeny. *Systematic Biology* **51**, 673-688.

876 Jakobsson M, Rosenberg NA (2007) CLUMPP: a cluster matching and permutation  
 877 program for dealing with label switching and multimodality in analysis of  
 878 population structure. *Bioinformatics* **23**, 1801-1806.

879 Jones OR, Wang J (2010) COLONY: a program for parentage and sibship inference  
 880 from multilocus genotype data. *Molecular Ecology Resources* **10**, 551-555.

881 Jost L (2008) GST and its relatives do not measure differentiation. *Molecular Ecology*  
 882 **17**, 4015-4026.

883 Kalinowski ST (2005) hp-rare 1.0: a computer program for performing rarefaction on  
 884 measures of allelic richness. *Molecular Ecology Notes* **5**, 187-189.

885 Kalinowski ST, Wagner AP, Taper ML (2006) ML-RELATE: a computer program for  
 886 maximum likelihood estimation of relatedness and relationship. *Molecular*  
 887 *Ecology Notes* **6**, 576-579.

888 Katoh K, Standley DM (2013) MAFFT Multiple sequence alignment software version  
 889 7: improvements in performance and usability. *Molecular Biology and Evolution*  
 890 **30**, 772-780.

891 Kühnel S, Reinhard S, Kupfer A (2010) Evolutionary reproductive morphology of  
 892 amphibians: an overview. *Bonn Zoological Bulletin* **57**, 119-126.

893 Leimu R, Mutikainen PIA, Koricheva J, Fischer M (2006) How general are positive  
 894 relationships between plant population size, fitness and genetic variation?  
 895 *Journal of Ecology* **94**, 942-952.

896 Lewis PO, Zaykin D (2000) Genetic data analysis: computer program for the analysis of  
 897 allelic data, version 1.0. (d15), University of Connecticut, Storrs, Connecticut,  
 898 USA.

899 MacLeod A, Rodríguez A, Vences M, Orozco-terWengel P, García C, Trillmich F *et al.*  
900 (2015) Hybridization masks speciation in the evolutionary history of the  
901 Galápagos marine iguana. *Proceedings of the Royal Society B* **282**, 20150425.

902 Mantel N (1967) The detection of disease clustering and a generalized regression  
903 approach. *Cancer Research* **27**, 209-220.

904 Martínez-Solano I, Teixeira J, Buckley D, García-París M (2006) Mitochondrial DNA  
905 phylogeography of *Lissotriton boscai* (Caudata, Salamandridae): evidence for  
906 old, multiple refugia in an Iberian endemic. *Molecular Ecology* **15**, 3375-3388.

907 Milá B, Carranza S, Guillaume O, Clobert J (2010) Marked genetic structuring and  
908 extreme dispersal limitation in the Pyrenean brook newt *Calotriton asper*  
909 (Amphibia: Salamandridae) revealed by genome-wide AFLP but not mtDNA.  
910 *Molecular Ecology* **19**, 108-120.

911 Monsen KJ, Blouin MS (2004) Extreme isolation by distance in a montane frog *Rana*  
912 *cascadae*. *Conservation Genetics* **5**, 827-835.

913 Nosil P, Funk DJ, Ortiz-Barrientos D (2009) Divergent selection and heterogeneous  
914 genomic divergence. *Molecular Ecology* **18**, 375-402

915 Orozco-terWengel P, Barbato M, Nicolazzi E, Biscarini F, Milanesi M, Davies W, *et al.*  
916 (2015) Revisiting demographic processes in cattle with genome-wide population  
917 genetic analysis. *Frontiers in genetics* **6**, 191.

918 Paetkau D, Slade R, Burden M, Estoup A (2004) Genetic assignment methods for the  
919 direct, real-time estimation of migration rate: a simulation-based exploration of  
920 accuracy and power. *Molecular Ecology* **13**, 55-65.

921 Paz A, Ibáñez R, Lips KR, Crawford AJ (2015) Testing the role of ecology and life  
922 history in structuring genetic variation across a landscape: a trait-based  
923 phylogeographic approach. *Molecular Ecology* **24**, 3723-3737.

924 Peakall R, Smouse PE (2006) GENALEX 6: genetic analysis in Excel. Population  
 925 genetic software for teaching and research. *Molecular Ecology Notes* **6**, 288-  
 926 295.

927 Piry S, Luikart G, Cornuet JM (1999) BOTTLENECK: A computer program for  
 928 detecting recent reductions in the effective population size using allele frequency  
 929 data. *Journal of Heredity* **90**(4), 502-503.

930 Piry S, Alapetite A, Cornuet J-M, Paetkau D, Baudouin L, Estoup A (2004)  
 931 GENECLASS2: a software for genetic assignment and first-generation migrant  
 932 detection. *Journal of Heredity* **95**, 536-539.

933 Plummer M, Best N, Cowles K, Vines K (2006) Coda: convergence diagnosis and  
 934 output analysis for MCMC. *R news* **6**, 7-11.

935 Pritchard JK, Stephens M, Donnelly P (2000) Inference of population structure using  
 936 multilocus genotype data. *Genetics* **155**, 945-959.

937 Queller DC, Goodnight KF (1989) Estimating relatedness using genetic markers.  
 938 *Evolution* **43**, 258-275.

939 Rambaut A, Drummond A (2007) *Tracer v1.5* <<http://beast.bio.ed.ac.uk/Tracer>>.

940 Recuero E, Canestrelli D, Vörös J, Szabó K, Poyarkov NA, Arntzen JW *et al.* (2012)  
 941 Multilocus species tree analyses resolve the radiation of the widespread *Bufo*  
 942 *bufo* species group (Anura, Bufonidae). *Molecular Phylogenetics and Evolution*  
 943 **62**, 71-86.

944 Romiguier J, Gayral P, Ballenghien M, Bernard A, Cahais V, Chenuil A *et al.* (2014)  
 945 Comparative population genomics in animals uncovers the determinants of  
 946 genetic diversity. *Nature* **515**, 261-263.

947 Rosenberg NA (2004) DISTRUCT: a program for the graphical display of population  
 948 structure. *Molecular Ecology Notes* **4**, 137-138.



949 Rousset F (1997) Genetic differentiation and estimation of gene flow from F-statistics  
950 under isolation by distance. *Genetics* **145**, 1219-1228.

951 Rousset F (2008) Genepop'007: a complete re-implementation of the genepop software  
952 for Windows and Linux. *Molecular Ecology Resources* **8**, 103-106.

953 Savage WK, Fremier AK, Bradley Shaffer H (2010) Landscape genetics of alpine Sierra  
954 Nevada salamanders reveal extreme population subdivision in space and time.  
955 *Molecular Ecology* **19**, 3301-3314.

956 Slatkin M (1994) Gene flow and population structure. In: *Ecological genetics* (ed. LA  
957 R), pp. 3-17. Princeton University Press, Princeton, New Jersey.

958 Šmíd J, Carranza S, Kratochvíl L, Gvoždík V, Nasher AK, Moravec J (2013) Out of  
959 Arabia: a complex biogeographic history of multiple vicariance and dispersal  
960 events in the gecko genus *Hemidactylus* (Reptilia: Gekkonidae). *PLoS ONE* **8**,  
961 e64018.

962 Smith MA, Green DM (2005) Dispersal and the metapopulation paradigm in amphibian  
963 ecology and conservation: are all amphibian populations metapopulations?  
964 *Ecography* **28**, 110-128.

965 Spear SF, Peterson CR, Matocq MD, Storfer A (2005) Landscape genetics of the  
966 blotched tiger salamander (*Ambystoma tigrinum melanostictum*). *Molecular*  
967 *Ecology* **14**, 2553-2564.

968 Steinfartz S, Weitere M, Tautz D (2007) Tracing the first step to speciation: ecological  
969 and genetic differentiation of a salamander population in a small forest.  
970 *Molecular Ecology* **16**, 4550-4561.

971 Storfer A, Mech S, Reudink M, Lew K (2013) Inbreeding and strong population  
972 subdivision in an endangered salamander. *Conservation Genetics*, 1-15.

973 Storz JF, Beaumont MA (2002) Testing for genetic evidence of population expansion  
 974 and contraction: an empirical analysis of microsatellite DNA variation using a  
 975 hierarchical bayesian model. *Evolution* **56**, 154-166.

976 Sunny A, Monroy-Vilchis O, Fajardo V, Aguilera-Reyes U (2014) Genetic diversity  
 977 and structure of an endemic and critically endangered stream river salamander  
 978 (Caudata: *Ambystoma leorae*) in Mexico. *Conservation Genetics* **15**, 49-59.

979 Szulkin M, Stopher KV, Pemberton JM, Reid JM (2013) Inbreeding avoidance,  
 980 tolerance, or preference in animals? *Trends in ecology & evolution* **28**, 205-211..

981 Tallmon DA, Koyuk A, Luikart G, Beaumont MA (2008) COMPUTER PROGRAMS:  
 982 onesamp: a program to estimate effective population size using approximate  
 983 Bayesian computation. *Molecular Ecology Resources* **8**, 299-301.

984 Templeton AR, Shaw K, Routman E, Davis SK (1990) The genetic consequences of  
 985 habitat fragmentation. *Annals of the Missouri Botanical Garden* **77**, 13-27.

986 Tregenza T, Wedell N (2002) Polyandrous females avoid costs of inbreeding. *Nature*  
 987 **415**, 71–73.

988 Valbuena-Ureña E, Amat F, Carranza S (2013) Integrative phylogeography of  
 989 *Calotriton* newts (Amphibia, Salamandridae), with special remarks on the  
 990 conservation of the endangered Montseny brook newt (*Calotriton arnoldi*).  
 991 *PLoS ONE* **8**, e62542.

992 Valbuena-Ureña E, Steinfartz S, Carranza S (2014) Characterization of microsatellite  
 993 loci markers for the critically endangered Montseny brook newt (*Calotriton*  
 994 *arnoldi*). *Conservation Genetics Resources* **6**, 263-265.

995 Van Oosterhout C, Hutchinson WF, Wills DPM, Shipley P (2004) Micro-checker:  
 996 software for identifying and correcting genotyping errors in microsatellite data.  
 997 *Molecular Ecology Notes* **4**, 535-538.

998 Veith M, Kosuch J, Vences M (2003) Climatic oscillations triggered post-Messinian  
 999 speciation of Western Palearctic brown frogs (Amphibia, Ranidae). *Molecular*  
 1000 *Phylogenetics and Evolution* **26**, 310-327.

1001 Velo-Antón G, Parra JL, Parra-Olea G, Zamudio KR (2013) Tracking climate change in  
 1002 a dispersal-limited species: reduced spatial and genetic connectivity in a  
 1003 montane salamander. *Molecular Ecology* **22**, 3261-3278.

1004 Waples RS, Do C (2008) LDNE: a program for estimating effective population size  
 1005 from data on linkage disequilibrium. *Molecular Ecology Resources* **8**, 753-756.

1006 Weir BS, Cockerham CC (1984) Estimating F-statistics for the analysis of population  
 1007 structure. *Evolution* **38**, 1358-1370.

1008

1009 Table 1. Estimates of genetic parameters for each *Calotriton arnoldi* population and  
 1010 cluster defined by STRUCTURE analysis, and for the four *C. asper* populations. Values  
 1011 represent averages across 24 loci. N, sample size; A, number of alleles per locus; Ar,  
 1012 allelic richness; PA, number of private alleles; PAAr, allelic richness of private alleles;  
 1013  $H_O$ , observed heterozygosity;  $H_E$ , expected heterozygosity;  $F_{IS}$ , inbreeding coefficient.  
 1014 Values in bold indicate statistical significance after Bonferroni correction.

1015 Table 2. Genetic differentiation among populations. Pairwise  $F_{ST}$ , below the diagonal;  
 1016 D estimator values above the diagonal. All  $P$  values were significant ( $P < 0.001$ ).

1017 Table 3. Estimates of effective population size ( $N_e$ ) for each population and cluster of  
 1018 *Calotriton arnoldi* and for the four *C. asper* populations, calculated with three  
 1019 programs: LDNe, ONeSAMP and COLONY; estimations of the upper and lower 95%  
 1020 CI estimates for each method are indicated. Relationship indicates the percentage of  
 1021 individual relatedness within each population and cluster.

1022 Table S1. Specimens of *Calotriton* included in the molecular analyses. For all 24  
 1023 specimens newly sequenced in the present study, we provide their taxonomic  
 1024 identification, sample code and GenBank accession numbers. Population and  
 1025 corresponding locality are shown in the map from Figure 1A.

1026 Table S2. Characterization of the full set of 24 applied microsatellite loci for *Calotriton*  
 1027 *arnoldi*. Loci are grouped by multiplex combinations used for amplification. Locus  
 1028 name, primer sequence, direction (F is forward, R is reverse), annealing temperature of  
 1029 the primer for PCRs, microsatellite motif, amplified fragment size range, number of  
 1030 alleles, labeling dye, and references are provided.

1031 Table S3. Prior distributions used for the MsVar analysis.  $N_0$ = current effective  
 1032 population size,  $N_t$ = ancestral effective population size,  $t$ = time of the change from  $N_0$  to

1033  $N_t$ , and  $m$ = mutation rate.  $M$  is the mean of a parameter and  $V$  its variance. Means of  
 1034 means and variances of means for the hyperpriors were the same as for the mean and  
 1035 variance of each parameter in the priors, and the hyperprior's mean of variances and  
 1036 variance of variances were 0 and 0.5, respectively.

1037 Table S4. Estimates of genetic parameters for each population and locus.  $N$ , sample  
 1038 size;  $A$ , number of alleles per locus;  $A_r$ , allelic richness;  $PA$ , number of private alleles;  
 1039  $PA_r$ , allelic richness of private alleles;  $H_O$ , observed heterozygosity;  $H_E$ , expected  
 1040 heterozygosity;  $F_{IS}$ , inbreeding coefficient.

1041 Table S5. Estimates of genetic diversity for each of the four *Calotriton asper*  
 1042 populations and loci used in this study.  $N$ , sample size;  $A$ , number of alleles per locus;  
 1043  $H_O$ , observed heterozygosity;  $H_E$ , expected heterozygosity;  $F_{IS}$ , inbreeding coefficient.  
 1044 None of the  $F_{IS}$  values are statistical significant after Bonferroni correction.

1045 Table S6. Results of the Wilcoxon signed-rank test for the comparison of genetic  
 1046 diversity estimates in terms of differences in heterozygosity estimates ( $H_E$  and  $H_O$ ) and  
 1047 number of alleles per locus ( $A$ ) between *C. arnoldi* and the four *C. asper* populations. In  
 1048 bold are the significant  $p$ -value after Bonferroni correction for multiple comparisons.

1049 Table S7. Values used in isolation by distance (IBD) analysis. Measure of genetic  
 1050 differentiation  $F_{ST} / (1 - F_{ST})$  below the diagonal; logarithmic geographic distances in km  
 1051 above the diagonal.

1052 Table S8. Recent migration rate estimations between *Calotriton arnoldi* populations  
 1053 within eastern and western sectors.

1054 Table S9. Highest posterior probabilities for the demographic parameters inferred with  
 1055 MSVAR.  $N_{\theta}$ = current effective population size,  $N_t$ = ancestral effective population size,

1056  $t$ = time of the change from  $N_0$  to  $N_t$ . HPD Low and HPD Up are the lower and upper  
1057 highest posterior density interval, respectively. Values in the table are in log(10) scale,  
1058 e.g. 2 corresponds to 100 and 4 to 10,000.

1059 Figure 1. A, The distribution range of the Montseny brook newt, *Calotriton arnoldi*.  
1060 Populations located in the eastern sector and in the western sector are separated by the  
1061 Tordera river valley (Valbuena-Ureña *et al.* 2013). All localities have been sampled for  
1062 this study. Shade indicates the actual distribution range of *C. asper*. Locations of the *C.*  
1063 *asper* populations used in this study are also shown (ACH: Ibón de Acherito; BAS:  
1064 Bassies; IRA: Irati; PER: Ibón de Perramó; VAL: Barranco de Valdragás). B, Bayesian  
1065 Inference tree of *Calotriton* inferred using BEAST with the concatenated datasets. A list  
1066 of details of all the specimens is presented in Supplementary Table S1. Black-filled  
1067 circle indicates  $pp > 0.95$  in the BEAST analysis. Ages of some relevant nodes are  
1068 shown by the nodes in with the 95% HPD underneath between square brackets.

1069 Figure 2. A, Results of Bayesian clustering and individual assignment analysis obtained  
1070 with STRUCTURE after running the program with all populations (above) and by  
1071 sector (below); vertical bars delimit sampling locations. B, inference for the best value  
1072 of  $K$  based on the  $\Delta K$  method among runs for all populations and by sector.

1073 Figure 3. Demographic analysis using MSVAR. For populations A1 to A3 and B1 to  
1074 B3, their current effective population size is shown (plots A and B), the ancestral  
1075 effective population size before the bottleneck (plots C and D), and the time of the  
1076 bottleneck (plots E and F). The posterior distributions of each parameter for the A  
1077 populations are shown in shades of dark grey, and for the B populations in shades of  
1078 light grey. For each population three distributions are shown for each parameter, as each

1079 population was analyzed using three alternative priors. The x-axis is in log(10) scale, for  
1080 example, 2 represents 100, and 4 represents 10,000.

1081 Figure S1. Population structure based on factorial correspondence analysis of all  
1082 populations. Each square represents an individual multilocus genotype, colored  
1083 according to the location from where it was sampled.

1084 Figure S2. Isolation by distance between populations. Blue symbols represent between  
1085 sectors comparisons; red and black symbols represent between populations comparisons  
1086 of eastern and western sectors, respectively.

1087 Figure S3. Distribution of ratios of  $N_t/N_0$  for each population. For each population three  
1088 distributions are shown representing the ratio of the ancestral effective population size  
1089 ( $N_t$ ) divided by the current effective population size ( $N_0$ ). Under a demographically  
1090 stable population, the effective population size should be centered around 1 (i.e.  $N_t/N_0$   
1091  $\sim 1$ ), however, the distributions for each of the three analyses for the populations show  
1092 values larger than 1 — indicative of a decrease in effective population size consistent  
1093 with a bottleneck.

1094 Figure S4. Mean within-population pairwise relatedness values ( $r_{pq}$ ) between  
1095 populations of eastern (A) and western (B) sectors. Red bars represent the upper (U) and  
1096 lower (L) confidence intervals with 95 % confidence with a null distribution generated  
1097 with 999 permutations. Blue bars represent the observed kinship mean conducted with  
1098 999 bootstraps.

	Grouping	N	A	Ar	PA	PAAr	H <sub>O</sub>
<i>C. arnoldi</i>	Population						
	A1	23	4.167	4.167	7	0.311	0.545
	A2	27	4.042	3.954	5	0.214	0.526
	A3	27	4.292	4.222	5	0.215	0.560
	B1	25	3.542	3.500	3	0.137	0.467
	B2	28	2.917	2.860	2	0.087	0.371
	B3	26	1.792	1.768	2	0.079	0.230
	B4	4	2.333	-	0	-	0.438
	Clusters						
	Eastern	77	4.167	4.112	75	3.157	0.544
	A1-A2	50	4.099	4.052	19	0.746	0.535
	Western	83	2.724	2.703	38	1.646	0.359
	B1-B2-B4	57	3.150	3.162	19	0.750	0.418
<i>C. asper</i>	Population						
	Ibón de Perramó	48	3.947	4.210	19	0.710	0.438
	Barranco de Valdragás	39	6.000	6.010	18	0.770	0.641
	Ibón de Acherito	40	5.895	5.940	18	0.520	0.593
	Bassies	162	4.071	5.690	33	1.130	0.500

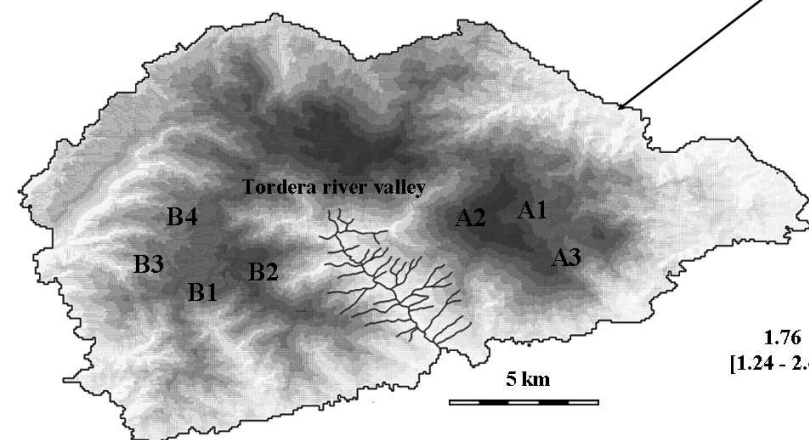
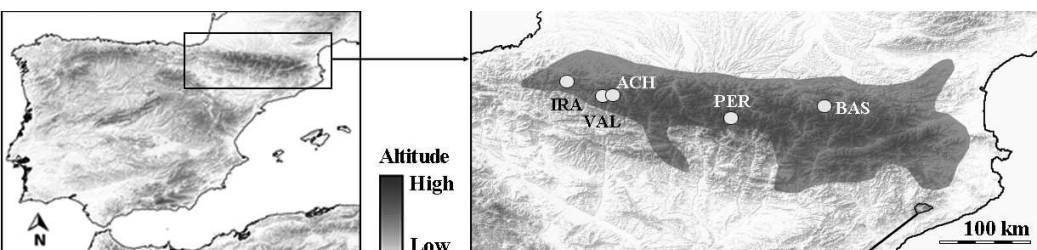


$H_E$	$F_{IS}$
0.538	0.017
0.516	-0.015
0.559	-0.007
0.469	-0.005
0.380	0.028
0.197	-0.121
0.433	-0.023
0.538	<b>0.090</b>
0.526	0.029
0.352	<b>0.184</b>
0.423	<b>0.073</b>
0.444	0.025
0.619	-0.022
0.588	0.005
0.558	0.107

$F_{ST}/D$	A1	A2	A3	B1	B2	B3	B4
A1	-	0.131	0.243	0.814	0.816	0.852	0.782
A2	0.086	-	0.299	0.855	0.868	0.877	0.822
A3	0.151	0.178	-	0.806	0.801	0.858	0.762
B1	0.457	0.473	0.443	-	0.100	0.249	0.122
B2	0.509	0.524	0.491	0.096	-	0.248	0.146
B3	0.614	0.617	0.599	0.336	0.372	-	0.305
B4	0.443	0.460	0.419	0.109	0.145	0.488	-

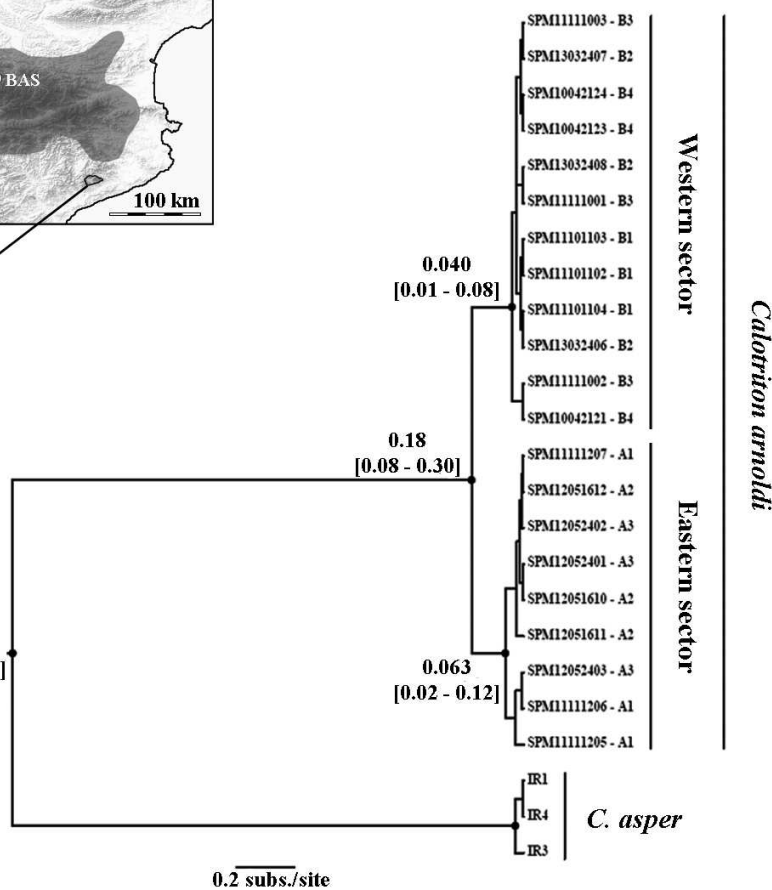
		LDNe			OneSamp		
<i>C. arnoldi</i>	Population	$N_e$	95% CIs		$N_e$	95% CIs	
	A1	342.30	77.00	infinite	27.65	24.51	34.81
	A2	49.40	32.20	93.20	33.94	29.94	41.89
	A3	142.10	61.80	infinite	36.85	33.33	43.20
	B1	55.80	34.10	126.40	31.59	27.77	40.69
	B2	62.20	27.50	15091.10	36.39	30.46	53.44
	B3	7.30	2.40	21.70	14.97	12.61	19.61
	B4	infinite	infinite	infinite	5.54	4.87	6.64
	Clusters						
<i>C. asper</i>	A1-A2	44.50	36.00	56.50	85.95	66.52	127.10
	B1-B2-B4	30.00	23.60	39.00	80.14	55.44	157.01
	Population						
	Ibón de Perramó	349.80	100.30	infinite	42.80	33.96	62.07
	Barranco de Valdragás	1293.00	201.40	infinite	41.41	35.29	58.22
<i>C. asper</i>	Ibón de Acherito	172.80	89.50	1078.90	60.80	46.42	99.78
	Bassies	92.00	61.90	149.50	28.73	21.65	41.06

COLONY			Relationship			
$N_e$	95% CIs		Unrelated	Half Siblings	Full Siblings	Parent Offspring
46.00	26.00	90.00	91.70	7.51	0.40	0.40
40.00	25.00	71.00	90.31	7.12	0.85	1.71
44.00	28.00	80.00	91.17	7.98	0.28	0.57
35.00	20.00	68.00	86.33	12.00	0.67	1.00
31.00	18.00	57.00	81.75	13.23	1.85	3.17
13.00	7.00	30.00	68.31	8.00	12.31	11.38
-	-	-	100	-	-	-
60.00	41.00	92.00	84.16	14.37	0.57	0.90
42.00	27.00	66.00	80.89	15.91	1.50	1.69
40.00	26.00	65.00	84.13	12.68	1.60	1.60
58.00	37.00	98.00	90.69	8.50	0.40	0.40
68.00	44.00	111.00	88.85	9.62	0.51	1.03
72.00	53.00	100.00	78.02	16.10	3.57	2.31



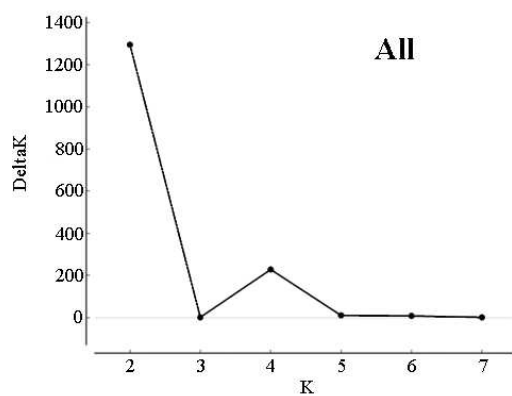
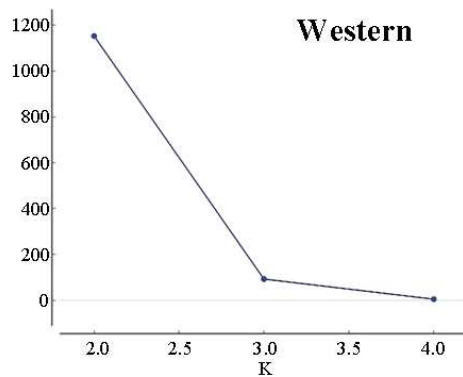
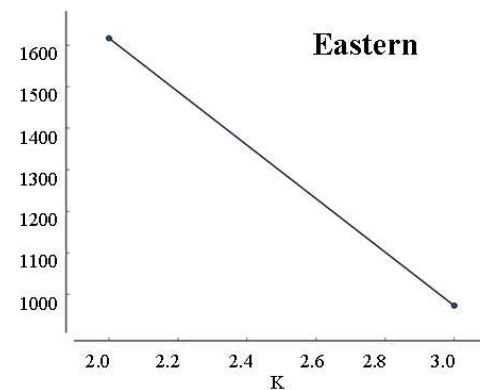
**A**

**B**



**A****Western sector****Eastern sector***B1**B2**B3**B4**A1**A2**A3***B**

$$\Delta K = \text{mean}(|L''(K)|) / \text{sd}(L(K))$$

**All****Western****Eastern**

